CORA Cork Open Research Archive
Cartlann Taighde Oscailte Chorcaí

Title	Two-dimensional materials and their role in emerging electronic and photonic devices
Authors	O'Dwyer, Colm;Walsh, Lee A.;Gity, Farzan;Bhattacharjee, Shubhadeep;Hurley, Paul K.
Publication date	2018-12-01
Original Citation	O'Dwyer, C., Walsh, L. A., Gity, F., Bhattacharjee, S. and Hurley, P. K. (2018) 'Two-Dimensional Materials and Their Role in Emerging Electronic and Photonic Devices', The Electrochemical Society Interface, 27(4), pp. 53-58. doi: 10.1149/2.F06184if
Type of publication	Article (peer-reviewed)
Link to publisher's version	http://interface.ecsdl.org/content/27/4/53.abstract - 10.1149/2.F06184if
Rights	© ECS 2018
Download date	2026-10-30 08:13:55
Item downloaded from	https://hdl.handle.net/10468/7225

UCC
University College Cork, Ireland
Coláiste na hOllscoile Corcaigh

Two-Dimensional Materials and Their Role in Emerging Electronic and Photonic Devices

by Colm O'Dwyer, Lee A. Walsh, Farzan Gity, Shubhadeep Bhattacharjee, and Paul K. Hurley

As the scaling of semiconducting devices in integrated circuits approaches dimensions less than 10 nm, the emphasis for future technologies has moved towards improved energy efficiency and the use of three dimensional (3D) integration schemes[1] to achieve an increased density of devices per unit area. For many of these applications there is a need to explore new semiconducting materials which allow flexibility in electronic and optical properties, and can also be processed at reduced temperatures, which allows their integration above conventional silicon based integrated circuits. One class of materials that demonstrates considerable promise for these emerging applications is van der Waals bonded two dimensional (2D) semiconductors. The study of these 2D layered material systems is not new, with studies dating back to the 1920s[2] and the identification of monolayers and bi-layers of MoS_2 in the 1960s.[3] What is particularly exciting about this general class of semiconductors is that they have a range of energy gaps which span from semi-metals through to wide bandgap semiconductors and as a consequence have potential applications in electronic devices, sensors, through to applications in flexible electronics, photovoltaics, and the light emitting diodes.

In terms of the potential applications, we emphasize 2D devices and structures where the specific properties of some 2D materials open the potential for novel or improved device performance when compared to their bulk counterparts, based on new ways of growing heterostructures and junctions of 2D materials, and a brief toe-dip into the pool of intriguing physics that are beginning to be exploited in 2D materials systems.

Large Area Growth of 2D Layered Materials

Transition metal dichalcogenide (TMD) materials research has been primarily performed on geological or chemical vapor transport grown bulk crystals. While this material is appropriate for exploratory research, it's less suitable for the large-scale integration required for reproducible device fabrication. Large-area growth provided by methods like chemical vapor deposition (CVD)[4,5] or molecular beam epitaxy (MBE)[6-8] can provide reproducible, high-purity thin films in addition to enabling material tuning through doping or composition control. In the epitaxial growth of 3D materials, such as Si, covalent bonding between the deposited atoms and the dangling bonds at the substrate surface can only occur for atoms that are closely lattice matched. This results in the formation of defects at the interface and/or strain of the epitaxially grown film (epilayer) in-plane bonding (Fig. 1a). In 2D materials, covalent bonding exists within each monolayer but only weak van der Waals bonding between successive monolayers. As such, the inert nature of 2D materials minimizes the covalent bonding at the interface, and thus results in a strain-free growth despite lattice mismatch (Fig. 1b). This reduces the lattice matching requirements for 2D material growth and facilitates the growth of 2D materials heterostructures, and the integration of these materials into new devices.[9] Device design can focus on selecting materials with the desired electronic structure and properties.

MBE uses elemental precursors and the film is grown by impinging metal and chalcogen precursors onto a substrate at a

(continued on next page)

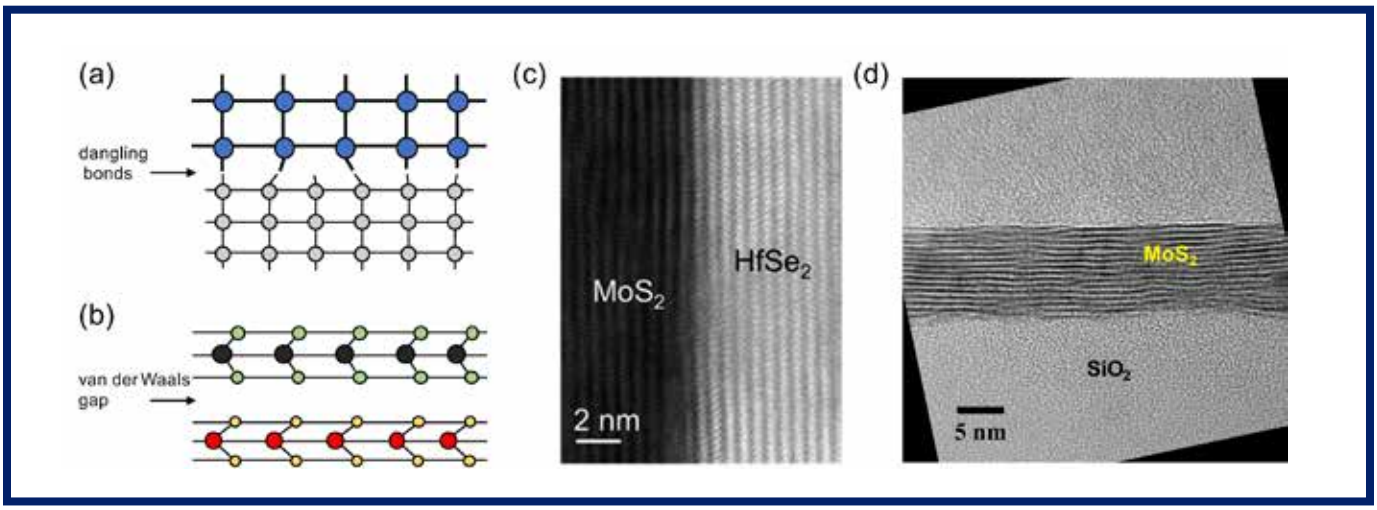


Fig. 1. *Schematic figures showing the impact of lattice mismatch in (a) conventional epitaxy where covalent bonding occurs at the interface, and (b) van der Waals epitaxy where only van der Waals bonding exists at the interface. (Reprinted with permission from Elsevier.[10]) (c) TEM image of MBE grown $HfSe_2$ on MoS_2. (Reprinted with permission from ACS.[11]) (d) TEM image of CVD grown MoS_2 on SiO_2.[12]*

Downloaded on 2018-12-14 to IP 80.233.45.30 address. See ecsdl.org/site/terms_use. © ECS 2018

controlled rate and temperature. In addition to the growth of binary TMDs, the use of elemental source materials in MBE allows for the growth of ternary alloys such as $MoSe_{2x}Te_{2(1-x)}$, or the introduction of substitutional dopants.[13,14] Heterostructure fabrication using various 2D materials has also been demonstrated with more than of 40% lattice mismatch between successive layers, such as $HfSe_2$ grown on MoS_2 (Fig. 1b).[7,11] This highlights that mismatch-induced strain is not a significant constraint. One of the primary issues with MBE grown material has been limited grain sizes, which lead to low carrier mobilities. However, a recent study has shown that this is a result of the TMD being grown with excessive material fluxes and growth rates.[15] By limiting the precursor flux and growth rate, grain nucleation is minimized which allows each nucleation point to grow slowly into a larger grain. The majority of MBE grown material has used inert, crystalline substrates. For integration into conventional fabrication, direct growth on a dielectric such as SiO_2 is necessary. This has been a focus recently with some initial work showing the ability to grow crystalline 2D materials directly on amorphous oxides at low temperatures.[16]

CVD growth can be achieved either through the conversion of metal-oxide precursors using a chalcogen vapor or through the use of metal-organic precursors in metal-organic CVD (MOCVD). In the case of MOCVD, the selective chemistry between the metal and chalcogen precursor helps to control the TMD growth. MOCVD grown TMDs have typically shown larger grain sizes due to the additional control provided by the precursor chemistry, and growth directly on oxides has been demonstrated. Wafer-scale growth with monolayer thickness control has been achieved for MoS_2 and WS_2,[17] while impurity levels can be reduced by refining the precursors.[18] In-situ doping during film growth has also been explored with some success even at monolayer thickness, e.g., Re or Mn-doped MoS_2.[19,20] One of the primary issues with CVD is the growth temperatures in state-of-the-art CVD growth are typically quite high, in excess of 700 °C, which is beyond the limits for back-end-of-line integration (<450 °C). But there have been successful demonstrations of low temperature CVD growth, such as the MoS_2 film shown in Fig. 1d.[12] This film still maintains the layered nature of TMDs while keeping the growth temperature below 500 °C.

Large area epitaxial growth has made significant strides towards device-quality material but there are still issues to address. Grain size improvement will lead to improved transport characteristics, while lowering growth temperature and growing directly on Si-compatible substrates will address some of the concerns regarding the integration of these materials into industrial fabrication processes.

Electron Devices

Due to the weak inter-planar van der Waals interactions TMDs can be exfoliated and/or naturally grown into atomically thin layers with virtually no surface roughness.[20,21] Furthermore, these materials can be "transferred/placed" on top of each other enabling extreme heterostructure engineering without the lattice mismatch restrictions typically encountered in bulk semiconductors.[22,23] These features point to the potential of using 2D semiconductors for ultra-scaled transistors owing to two key factors. First, the characteristic length of the transistor ($\lambda = \sqrt{\frac{\epsilon_s}{\epsilon_{ox}} t_{ch} t_{ox}}$), a measure of the smallest scalable channel length, is directly proportional to the channel body thickness.[24,25] Therefore, by exploiting the fundamental limit of monolayer channel body thickness, the research community has been able to demonstrate 1 nm gate length (5-10 nm channel length) field-effect transistors (FETs) without any short channel effects and high ON to OFF ratio (Fig. 2a).[26-28] It is important to note that these demonstrations are on simple planar architectures, thus circumventing the need for complicated 3D/FinFET device designs. Furthermore, the ultra-thin body 2D transistor does not suffer from the surface roughness (t) dependent mobility losses (t^{-6}) which are limiting carrier transport in etched thin films of bulk semiconductors.[29]

Recent reports indicate that the superior electrostatics and electron confinement effects offered by these lower dimensional semiconductors can also be leveraged to design a variety of sub-thermionic (kT/q) transistors operating at supply voltages of 0.5 V or below[30-34] (Fig. 2b). An example is shown in Fig. 2c which shows a composite hetero-junction 2D (MoS_2)/3D (Ge) tunnel FET exhibiting a sub-threshold slope <60 mV/dec for over 4 orders of magnitude in the drain-source current. In addition to logic elements, it is interesting to note recent reports[35] using 2D semiconductors as the active layer in a variety of next generation three- and two-terminal memory architectures.

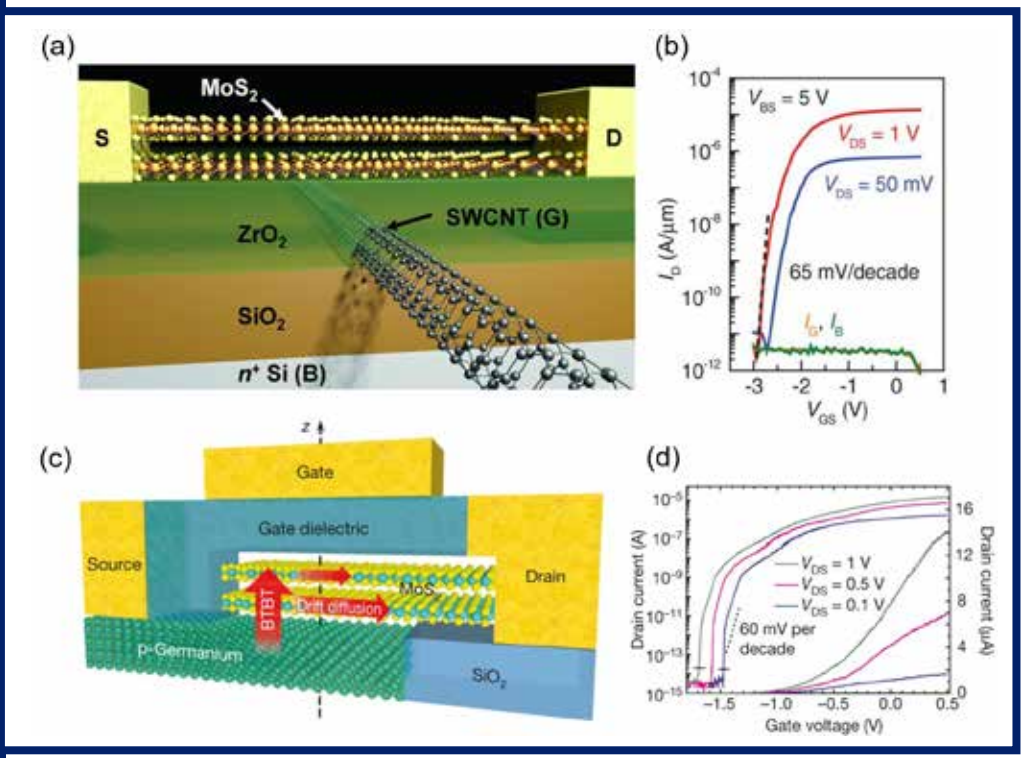


Fig. 2. *(a) A short gate length (1 nm, CNT) MoS_2 transistor demonstrating (b) high ON to OFF ratio and reasonable short channel effects. (Reprinted with permission from AAAS.[26]) (c) An MoS_2/Ge heterojunction tunnel FET demonstrating (d) sub-thermionic (sub-threshold slope <60 mV/dec) for 4 continuous decades. (Reprinted with permission from Nature Publishing Group.[30])*

Lateral 2D Heterojunctions in Electronic Devices

Graphene, as the probably the most ubiquitous 2D material, has proven to be a model and also accessible material system for making very small transistors, or at least electronic or optoelectronic devices with one physical dimension minimized. 2D materials can, in some cases, carry relatively high currents and some have bandgaps that are tunable by quantum effects, reduced dimensionality or interlayer gap tuning, among other mechanisms. Graphene suffers from conventional electronic structure as it has no bandgap, and often transistors

Downloaded on 2018-12-14 to IP 80.233.45.30 address. See ecsdl.org/site/terms_use. © ECS 2018

made from graphene are somewhat leaky, and difficult to maintain in an "off" state. Transistors based on 2D TMDs, discussed earlier, can show high on-off ratios in the current, but they too have drawbacks from conventional processing, layer stacking or contacting. Making a good voltage-biased p-n junction between different 2D TMDs is not a simple feat, especially as stacked junctions of different TMDs tend to be relatively weak junctions that are dependent on interlayer coupling strength[36] and necessitate good control over stacking orientation. One approach developed by Li et al.[37] was to grow MoS_2 on the edge of a 2D crystal of WSe_2 with an atomically sharp, abrupt junction, summarized in Fig. 3. It is a two-step process, that uses the first 2D TMD (WSe_2) grown by van der Waals epitaxy to grow the second 2D TMD (MoS_2) by edge epitaxy along the W growth front—importantly, this method avoids alloying, which is common in precursor based approaches to TMD phases. The key growth condition that avoided alloy formation was the control over the relative vapor quantity of MoO_3 and S during the MoS_2 growth; vertical MoS_2 dominates[38] and WS_2 at the interface that forms in excess S vapor is avoided.

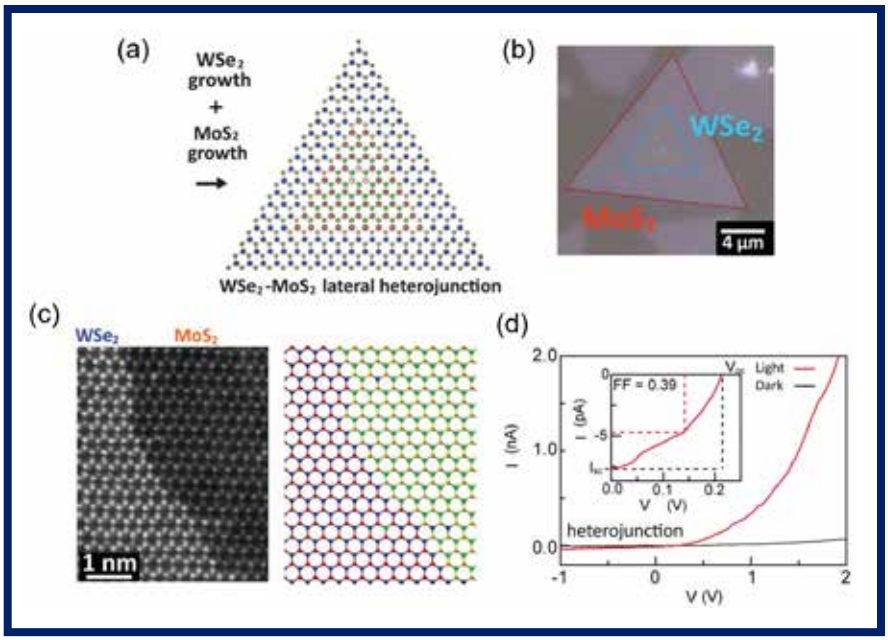


Fig. 3. *(a) Schematic illustration and (b) optical image of the sequential growth of the monolayer WSe_2-MoS_2 in-plane heterostructure. (c) High-resolution STEM of a WSe_2-MoS_2 in-plane heterostructure together with an atomic model of the heterointerface. (d) I-V curves showing the response of a p-n junction in the dark and a photovoltaic effect under illumination. (Adapted with permission from AAAS, 2015.)*

An exciting prospect for lateral p-n junction growth in nano- and monolayer electronics is the ability to have directly grown heterointerfaces that are sharp, well defined, and that the junction exhibits a depletion width, associated current rectification, and related photoresponses that include photovoltaic effects. Since this growth mode was published, other 2D TMD have been grown in this way to enable p-n junction and device formation, including lateral heterostructures of MoS_2/WS_2 and $WSe_2/MoSe_2$.

Optoelectronics with 2D Materials

In the case of optoelectronic devices, due to large local confinement of charge carriers within an atomically thin sheet, the excitonic binding energy of electron hole pairs are several times larger than the thermal noise, unlike bulk semiconductors.[39,40] This results in efficient photoluminescence and interesting optoelectronic devices such as photodetectors, LEDs and lasers based on strong excitonic effects.[41,42]

TMDs[43] and recently black phosphorus[44] in 2D form, and other materials,[45] are being studied as photodetectors[39] in photodiode or photoconductor regimes. Indeed, 2D TMD combinations with graphene (used as the channel material) have resulted in efficient phototransistors and other devices that rely on trapped charges induced or controlled by the illuminating photon flux.[46] Another approach based on heterogeneous combinations of 2D TMDs are devices based on photoexcitation of carriers (electrons and holes), whereby the carriers are trapped and accumulated in different layers from variations in the TMD workfunctions. In these devices, so-called indirect excitons are possible. Such excitons typically have long lifetimes, and their binding energy can be modified by tuning the interlayer gap between the semiconductor layers. Controlled doping and the formation of atomically sharp interfaces described earlier may also improve carrier separation for higher quantum efficiency.[47,48]

For light emitting devices, emission processes resulting from charge carrier recombination necessitates well-formed p-n junctions[48] with resistances much less than the individual p- and n-type electrodes to localize the current. Synthesizing and growing p- and n-type materials remains challenging even in cases where the stacking or growth is from a simpler chemical synthesis route. Direct epitaxy using CVD or related processes require efficient doping procedures that do not adversely influence the growth for either van der Waals stacked growth or indeed lateral in-plane heterojunctions. The possibility of growing both n- and p-type materials from the same 2D material is not ubiquitous to all 2D materials yet, and high output flux LEDs in 2D systems remain a technological challenge. Electrostatic (gate) tuning of effective doping in ambipolar 2D TMDs has enabled optoelectronic devices based on configurable p-n (and n-p) junctions with ideality factors greater than 2 as shown in Fig. 4. By controlling the gate voltage on both gates independently, the carrier concentration profile across the monolayer can be altered, which effectively dopes both sides into different (opposite) conducting regimes that enables current rectification like a diode. In the case where the junction barrier dominates over the Schottky barriers from the gate contacts, the Shockley relation,[49]

$$I = \frac{nV_T}{R_S} W\left[\frac{I_0 R_S}{nV_T}\exp\left(\frac{V_{ds} + I_0 R_S}{nV_T}\right)\right] - I_0$$

that includes the series bias resistance R_s, can accurately describe the junction behavior in a single amibipolar gate configurable 2D TMD optoelectronic device. Here, with $V_T = k_B T/q$ the thermal voltage at temperature T, k_B the Boltzmann constant, q is the electron charge. I_0 is the reverse-bias current, n is the diode ideality factor, and W is the Lambert W function.

While conventional LED fabrication by MBE or CVD methods can rely on refractive index tuning to control light extraction efficiency, 2D material systems with ultrasmall LED junctions may be limited to some degree by device packaging, but may be engineered to avoid back reflection, interfacial roughness scattering, or absorption losses in single molecule thick, 2D dimensions. One benefit of molecular-thick materials is their effective transparency, and in the right energy range, the ability to maximize interaction volume when pumped or probed by a light source.

To give another example of 2D materials in optoelectronics showing enhanced light matter interactions, Brittnel et al.[50] showed that two 2D materials are better than one. In that case, WSe_2 was sandwiched between graphene top and bottom layers, acting as conductive transparent electrodes. The heterostructure, sensitized by Au nanoparticles tuned for enhanced plasmonic absorption, showed enhanced photocurrent, light absorption and operation as a photovoltaic device. In this example, devices with just three layers placed into a vertically stacked structure, each a single molecule thick, had external quantum efficiencies of ~30%.

(continued on next page)

Downloaded on 2018-12-14 to IP 80.233.45.30 address. See ecsdl.org/site/terms_use. © ECS 2018

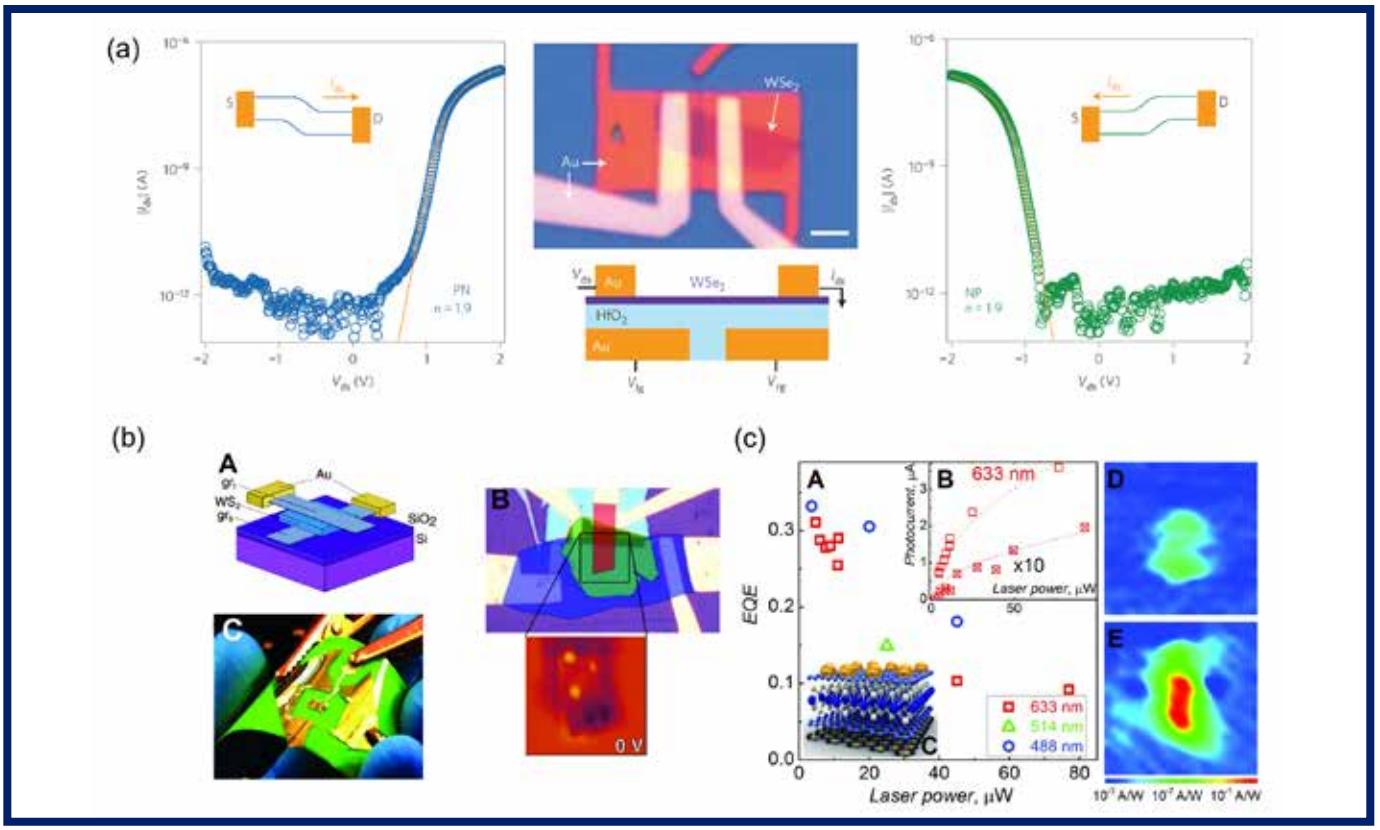


Fig. 4. *(a) Optical micrograph and schematic of a monolayer WSe_2 device controlled by two local gates (scale = 2 mm). I-V curves showing PN (blue circles) and NP (green circles) diode behavior from the dual-gated device as a function of V_{ds}. (Adapted with permission from Nature Publishing Group, 2014.) (b) Schematic (A), optical image (B) with top and bottom graphene electrodes shown in red and blue, and WS_2 is shown in green. Photo (C) of the device. (c) The external quantum efficiency (A) and photocurrent (B) of the devices which is a hBN/Gr/MoS_2/Gr (layers bottom to top) photovoltaic structure with gold nanoparticles on the top graphene layer for plasmonic absorption. (Adapted with permission from AAAS, 2013.)*

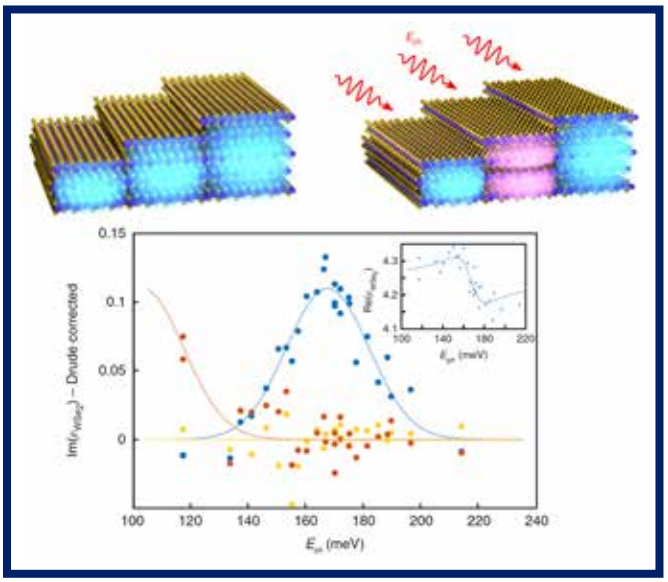


Fig. 5. *Charge carriers (blue) confined within a few-layer TMD material with different thickness. When a flake of a certain thickness is illuminated with light of energy E_{ph} with out-of-plane polarization, carriers can be excited from the ground state to the first excited state (pink) if the intersubband transition energy is resonant with E_{ph}. (b) Intersubband absorption spectra in few-layer WSe_2 for different excitation photon energies E_{ph} and layer numbers N. The blue dotted line fits the intersubband resonance at ~167.5 meV for N = 4 layer WSe_2. (Adapted with permission from Nature Publishing Group, 2018.)*

2D van der Waals Quantum Wells

As the opportunities for optoelectronics and the number of potentially useful 2D materials keep growing, heterostructures, in particular van der Waals heterostructures, offer a potentially fertile field for study and development. The reader will find many reviews on aspects of electron devices, materials growth, and optical properties in 2D materials in the current literature.[51]

In optoelectronics, however, 2D materials have not gained traction in the infrared and terahertz frequency ranges. Taking advantage of transitions between quantized states in semiconductor quantum wells, so-called intersubband transitions, potentially allows few-layer 2D TMD systems to absorb or emit in the terahertz frequencies. Minimizing the effects of diffusive interfaces and exploiting growth protocols that render lattice-mismatch a negligible issue in 2D analogs of quantum-well structures may improve matters. In principle, intersubband transitions are possible in any 2D material with a bandgap, but only very recently have experimentally verified intersubband transitions been reported in van der Waals quantum wells of WSe_2[52] where the absorption (separate to Drude absorption) is possible by electrostatically controlling the charge carrier density.

Schmidt et al.[52] used scanning near-field optical microscopy to locally probe intersubband resonances and absorption in gated few layer WSe_2 devices, showing particular absorption events as a function of the number of 2D layers in the material (see Fig. 5). Being able to enable intersubband absorption in these TMDs in few layer materials has some processing benefits, especially when few layers sulfide and selenides of transition metals (with a bandgap) are more readily grown by a larger number of growth methods; obtaining larger areas of true single layer 2D materials is currently a little more

Downloaded on 2018-12-14 to IP 80.233.45.30 address. See ecsdl.org/site/terms_use. © ECS 2018

difficult. Large area few-layer growth scenarios open up options for infrared lasers, detectors with 2D TMDs, especially when quantum-well structures can be integrated with Si-based electronics.

Outlook for 2D Material Future in Electronics and Photonics

Growing or obtaining 2D crystals from the hundreds of layered or van der Waals materials has opened up opportunities and possibilities in electronics and photonics that have been unprecedented compared to bulk materials. Semiconductors, dielectrics, conductors, and other material types are now all accessible in single-molecule thick crystals. Stacking of 2D layered materials and controlling interlayer coupling have uncovered unique physics that are being exploited and explored in nanoelectronics, while the unique band structure of compound materials has enabled a design freedom for novel optoelectronic devices with phenomena and functionalities that are different or not possible in corresponding bulk materials. Limits in doping control, resistivity, current densities, and stable off state, among many other parameters, are key to the eventual integration of 2D channel materials in electronics. Photonics and optoelectronics will benefit from development for high speed operation, including the development of light sources and detectors beyond UV and visible ranges.

© *The Electrochemical Society. DOI: 10.1149/2.F06184if.*

About the Authors



Colm O'Dwyer is a professor of chemical energy at the School of Chemistry, University College Cork, and principal investigator at Tyndall National Institute and the Environmental Research Institute, leading the Applied Nanoscience Group. His research investigates and develops functional materials and their properties for energy storage, solid state, and electrochemical science and technologies. He serves as chair of the ECS Electronics and Photonics Division, is on the ECS Board of Directors, and has organized over 25 ECS symposia in nanoscience, solid state science, and semiconductor electrochemistry. He is a fellow of the Institute of Physics. He may be reached at c.odwyer@ucc.ie.

https://orcid.org/0000-0001-7429-015X



Lee A. Walsh is a Marie Skłodowska-Curie postdoctoral research fellow at Tyndall National Institute. His research is focused towards understanding the fundamental processes which impact the epitaxial growth and integration issues for advanced materials into electronic devices, currently centered on 2D materials and topological insulators. He may be reached at lee.walsh@tyndall.ie.

https://orcid.org/0000-0002-6688-8626



Farzan Gity is a staff researcher in the Nanoelectronics Materials and Devices Group at Tyndall National Institute. Gity received his PhD in electronics engineering from University College Cork in 2013. He was then awarded the Irish Research Council Postdoctoral Fellowship for developing semimetal-based nanoelectronic devices. Gity was the principal investigator of the EU-H2020 SaSHa project at Tyndall. He also received the Science Foundation Ireland Technology Innovation and Development Award for integrating dissimilar materials for novel integrated sensor applications. His research interest is the heterogeneous-integration of low-dimensional materials (e.g., two-dimensional and (poly)crystalline III-V and group IV materials for advanced nanoelectronics and nanophotonics applications). He may be reached at farzan.gity@tyndall.ie.

https://orcid.org/0000-0003-3128-1426



Shubhadeep Bhattacharjee is a postdoctoral researcher in the Nano Materials and Devices Group at Tyndall National Institute, where his research focuses on nonvolatile memories. He received his PhD (2018) from the Indian Institute of Science, Bangalore, where he developed device architectures and material processing strategies for high-performance sub-thermionic transistors and optoelectronic devices based on two-dimensional materials. He may be reached at s.bhattacharjee@tyndall.ie.

https://orcid.org/0000-0002-5813-033X



Paul K. Hurley is a senior research scientist at Tyndall National Institute, and a research professor in the Department of Chemistry at University College Cork. Hurley leads a research team exploring alternative semiconductor materials and device structures aimed at improving the energy efficiency in the next generation of logic devices. In particular the group is working on III-V and 2D (e.g., MoS_2, WSe_2) semiconductors and their interfaces with metals and oxides that will form the heart of logic devices incorporating these materials. The group is also researching the use of metal-oxide-semiconductor (MOS) systems for the creation of solar fuels through water-splitting reactions. He may be reached at paul.hurley@tyndall.ie.

https://orcid.org/0000-0001-5137-721X

References

1. P. Batude, T. Ernst, J. Arcamone, G. Arndt, P. Coudrain, and P. E. Gaillardon, *IEEE J. Emerg. Sel. Topics Circuits Syst.*, **2**, 714 (2012).
2. R. G. Dickinson and L. Pauling, *J. Am. Chem. Soc.*, **45**, 1466 (1923).
3. R. F. Frindt, *J. Appl. Phys.*, **37**, 1928 (1966).
4. S. M. Eichfeld, L. Hossain, Y. C. Lin, A. F. Piasecki, B. Kupp, A. G. Birdwell, R. A. Burke, N. Lu, X. Peng, J. Li, A. Azcatl, S. McDonnell, R. M. Wallace, M. J. Kim, T. S. Mayer, J. M. Redwing, and J. A. Robinson, *ACS Nano*, **9**, 2080 (2015).
5. M. O'Brien, N. McEvoy, N. Hallam, H. Kim, N. C. Berner, D. Hanlon, K. Lee, J. N. Coleman, and G. S. Duesberg, *Sci. Rep.*, **4**, 7374 (2014).
6. L. A. Walsh, R. Yue, Q. Wang, A. T. Barton, R. Addou, C. M. Smyth, H. Zhu, J. Kim, L. Colombo, M. J. Kim, R. M. Wallace, and C. L. Hinkle, *2D Mater.*, **4**, 025044 (2017).
7. S. Vishwanath, X. Y. Liu, S. Rouvimov, L. Basile, N. Lu, A. Azcatl, K. Magno, R. M. Wallace, M. Kim, J. C. Idrobo, J. K. Furdyna, D. Jena, and H. G. Xing, *J. Mater. Res.*, **31**, 900 (2016).
8. L. A. Walsh, R. Addou, R. M. Wallace, and C. L. Hinkle, in *Molecular Beam Epitaxy: From Research to Mass Production*, Second ed., M. Henini, Editor, p. 515, Elsevier, New York (2018).
9. L. A. Walsh and C. L. Hinkle, *Appl. Mater. Today*, **9**, 504 (2017).
10. A. Koma, *J. Cryst. Growth*, **201**, 236 (1999).
11. R. Yue, A. T. Barton, H. Zhu, A. Azcatl, L. F. Pena, J. Wang, X. Peng, N. Lu, L. Cheng, R. Addou, S. McDonnell, L. Colombo, J. W. Hsu, J. Kim, M. J. Kim, R. M. Wallace, and C. L. Hinkle, *ACS Nano*, **9**, 474 (2015).

(continued on next page)

Downloaded on 2018-12-14 to IP 80.233.45.30 address. See ecsdl.org/site/terms_use. © ECS 2018

12. E. Coleman, S. Monaghan, F. Gity, M. Schmidt, J. Connolly, J. Lin, L. Walsh, K. Cherkaoui, K. O'Neill, N. McEvoy, C. O'Coileain, D. Buckley, C. O'Dwyer, P. K. Hurley, and G. S. Duesberg, Abstract 708, *The Electrochemical Society Meeting Abstracts,* Cancun, Mexico, September 30-October 4, 2018.
13. H. C. Diaz, Y. Ma, S. Kolekar, J. Avila, C. Chen, M. C. Asensio, and M. Batzill, *2D Mater.*, **4**, 025094 (2017).
14. S. N. Dong, X. Y. Liu, X. Li, V. Kanzyuba, T. Yoo, S. Rouvimov, S. Vishwanath, H. G. Xing, D. Jena, M. Dobrowolska, and J. K. Furdyna, *Apl Mater.*, **4,** 032601(2016).
15. R. Yue, Y. F. Nie, L. A. Walsh, R. Addou, C. P. Liang, N. Lu, A. T. Barton, H. Zhu, Z. F. Che, D. Barrera, L. X. Cheng, P. R. Cha, Y. J. Chabal, J. W. P. Hsu, J. Kim, M. J. Kim, L. Colombo, R. M. Wallace, K. Cho, and C. L. Hinkle, *2D Mater.*, **4**, 045019 (2017).
16. P. Paletti, R. Yue, C. L. Hinkle, and A. Seabaugh, *48th European Solid-State Device Research Conference*, Dresden, Germany (2018).
17. K. Kang, S. Xie, L. Huang, Y. Han, P. Y. Huang, K. F. Mak, C. J. Kim, D. Muller, and J. Park, *Nature*, **520**, 656 (2015).
18. X. Zhang, Z. Y. Al Balushi, F. Zhang, T. H. Choudhury, S. M. Eichfeld, N. Alem, T. N. Jackson, J. A. Robinson, and J. M. Redwing, *J. Electron. Mater.*, **45**, 6273 (2016).
19. K. Zhang, B. M. Bersch, J. Joshi, R. Addou, C. R. Cormier, C. Zhang, K. Xu, N. C. Briggs, K. Wang, S. Subramanian, K. Cho, S. K. Fullerton-Shirey, R. M. Wallace, P. M. Vora, and J. A. Robinson, *Adv. Funct. Mater.*, **28**, 1706950 (2018).
20. K. H. Zhang, S. M. Feng, J. J. Wang, A. Azcatl, N. Lu, R. Addou, N. Wang, C. J. Zhou, J. Lerach, V. Bojan, M. J. Kim, L. Q. Chen, R. M. Wallace, M. Terrones, J. Zhu, and J. A. Robinson, *Nano Lett.*, **15**, 6586 (2015).
21. A. K. Geim and I. V. Grigorieva, *Nature*, **499**, 419 (2013).
22. S. Z. Butler, S. M. Hollen, L. Cao, Y. Cui, J. A. Gupta, H. R. Gutierrez, T. F. Heinz, S. S. Hong, J. Huang, A. F. Ismach, E. Johnston-Halperin, M. Kuno, V. V. Plashnitsa, R. D. Robinson, R. S. Ruoff, S. Salahuddin, J. Shan, L. Shi, M. G. Spencer, M. Terrones, W. Windl, and J. E. Goldberger, *ACS Nano*, **7**, 2898 (2013).
23. A. Castellanos-Gomez, L. Vicarelli, E. Prada, J. O. Island, K. L. Narasimha-Acharya, S. I. Blanter, D. J. Groenendijk, M. Buscema, G. A. Steele, J. V. Alvarez, H. W. Zandbergen, J. J. Palacios, and H. S. J. van der Zant, *2D Mater.*, **1**, 025001 (2014).
24. F. Pizzocchero, L. Gammelgaard, B. S. Jessen, J. M. Caridad, L. Wang, J. Hone, P. Bøggild, and T. J. Booth, *Nat. Commun.*, **7**, 11894 (2016).
25. M. Bohr, *Tech. Dig. Int. Electron Devices Meet.*, p. 1, IEEE (2011).
26. S. B. Desai, S. R. Madhvapathy, A. B. Sachid, J. P. Llinas, Q. Wang, G. H. Ahn, G. Pitner, M. J. Kim, J. Bokor, C. Hu, H. S. P. Wong, and A. Javey, *Science*, **354**, 99 (2016).
27. A. Nourbakhsh, A. Zubair, R. N. Sajjad, A. Tavakkoli K. G, W. Chen, S. Fang, X. Ling, J. Kong, M. D. Dresselhaus, E. Kaxiras, K. K. Berggren, D. Antoniadis, and T. Palacios, *Nano Lett.*, **16**, 7798 (2016).
28. W. Cao, W. Liu, J. Kang, and K. Banerjee, *IEEE Electron Device Lett.*, **37**, 1497 (2016).
29. F. Gamiz, J. B. Roldán, P. Cartujo-Cassinello, J. A. López-Villanueva, and P. Cartujo, *J. Appl. Phys.*, **89**, 1764 (2001).
30. D. Sarkar, X. Xie, W. Liu, W. Cao, J. Kang, Y. Gong, S. Kraemer, P. M. Ajayan, and K. Banerjee, *Nature*, **526**, 91 (2015).
31. X. Wang, Y. Chen, G. Wu, D. Li, L. Tu, S. Sun, H. Shen, T. Lin, Y. Xiao, M. Tang, W. Hu, L. Liao, P. Zhou, J. Sun, X. Meng, J. Chu, and J. Wang, *2D Mater. Appl.*, **1**, 38 (2017).
32. F. A. McGuire, Y. C. Lin, K. Price, G. B. Rayner, S. Khandelwal, S. Salahuddin, and A. D. Franklin, *Nano Lett.*, **17**, 4801 (2017).
33. M. Si, C. J. Su, C. Jiang, N. J. Conrad, H. Zhou, K. D. Maize, G. Qiu, C. T. Wu, A. Shakouri, M. A. Alam, and D. Y. Peide, *Nat. Nanotechnol.*, **13**, 24 (2018).
34. S. Bhattacharjee, K. L. Ganapathi, S. Mohan, and N. Bhat, *Appl. Phys. Lett.*, **111**, 163501 (2017).
35. R. Ge, X. Wu, M. Kim, J. Shi, S. Sonde, L. Tao, Y. Zhang, J. C. Lee, and D. Akinwande, *Nano Lett.*, **18**, 434 (2017).
36. M.-H. Chiu, M.-Y. Li, W. Zhang, W.-T. Hsu, W.-H. Chang, M. Terrones, H. Terrones, and L.-J. Li, *ACS Nano*, **8**, 9649 (2014).
37. M.-Y. Li, Y. Shi, C.-C. Cheng, L.-S. Lu, Y.-C. Lin, H.-L. Tang, M.-L. Tsai, C.-W. Chu, K.-H. Wei, J.-H. He, W.-H. Chang, K. Suenaga, and L.-J. Li, *Science*, **349**, 524 (2015).
38. Y. Gong, J. Lin, X. Wang, G. Shi, S. Lei, Z. Lin, X. Zou, G. Ye, R. Vajtai, B. I. Yakobson, H. Terrones, M. Terrones, Beng K. Tay, J. Lou, S. T. Pantelides, Z. Liu, W. Zhou, and P. M. Ajayan, *Nat. Mater.*, **13**, 1135 (2014).
39. F. H. L. Koppens, T. Mueller, P. Avouris, A. C. Ferrari, M. S. Vitiello, and M. Polini, *Nat. Nanotechnol.*, **9**, 780 (2014).
40. G. Eda and S. A. Maier, *ACS Nano*, **7**, 5660 (2013).
41. O. Lopez-Sanchez, D. Lembke, M. Kayci, A. Radenovic, and A. Kis, *Nat. Nanotechnol.*, **8**, 497 (2013).
42. D. S. Tsai, K. K. Liu, D. H. Lien, M. L. Tsai, C. F. Kang, C. A. Lin, L. J. Li, and J. H. He, *ACS Nano*, **7**, 3905 (2013).
43. Q. H. Wang, K. Kalantar-Zadeh, A. Kis, J. N. Coleman, and M. S. Strano, *Nat. Nanotechnol.*, **7**, 699 (2012).
44. M. Buscema, D. J. Groenendijk, S. I. Blanter, G. A. Steele, H. S. J. van der Zant, and A. Castellanos-Gomez, *Nano Lett*, **14**, 3347 (2014).
45. F. Xia, H. Wang, D. Xiao, M. Dubey, and A. Ramasubramaniam, *Nat. Photonics*, **8**, 899 (2014).
46. K. Roy, M. Padmanabhan, S. Goswami, T. P. Sai, G. Ramalingam, S. Raghavan, and A. Ghosh, *Nat. Nanotechnol.*, **8**, 826 (2013).
47. F. Wang, Z. Wang, K. Xu, F. Wang, Q. Wang, Y. Huang, L. Yin, and J. He, *Nano Lett*, **15**, 7558 (2015).
48. R. Cheng, D. Li, H. Zhou, C. Wang, A. Yin, S. Jiang, Y. Liu, Y. Chen, Y. Huang, and X. Duan, *Nano Lett*, **14**, 5590 (2014).
49. B. W. H. Baugher, H. O. H. Churchill, Y. Yang, and P. Jarillo-Herrero, *Nat. Nanotechnol.*, **9**, 262 (2014).
50. L. Britnell, R. M. Ribeiro, A. Eckmann, R. Jalil, B. D. Belle, A. Mishchenko, Y.-J. Kim, R. V. Gorbachev, T. Georgiou, S. V. Morozov, A. N. Grigorenko, A. K. Geim, C. Casiraghi, A. H. C. Neto, and K. S. Novoselov, *Science*, **340**, 1311 (2013).
51. K. F. Mak and J. Shan, *Nat. Photonics*, **10**, 216 (2016).
52. P. Schmidt, F. Vialla, S. Latini, M. Massicotte, K.-J. Tielrooij, S. Mastel, G. Navickaite, M. Danovich, D. A. Ruiz-Tijerina, C. Yelgel, V. Fal'ko, K. S. Thygesen, R. Hillenbrand, and F. H. L. Koppens, *Nat. Nanotechnol.*, (2018) DOI: 10.1038/s41565-018-0233-9.

ECS arXiv™
a free preprint service for electrochemistry and solid state science and technology
COS CENTER FOR OPEN SCIENCE
powered by OSF Preprints
www.electrochem.org/ecsarxiv

Downloaded on 2018-12-14 to IP 80.233.45.30 address. See ecsdl.org/site/terms_use. © ECS 2018